

Electron Transfer across Polypeptides. 5. Rapid Rates of Electron Transfer between Os(II) and Co(III) in Complexes with Bridging Oligoprolines and Other Polypeptides

Stephan S. Isied,* Asbed Vassilian, Roy H. Magnuson, and Harold A. Schwarz*

Contribution from the Department of Chemistry, Rutgers, The State University of New Jersey, New Brunswick, New Jersey 08903, and Department of Chemistry, Brookhaven National Laboratory, Upton, New York 11973. Received February 20, 1985

Abstract: A series of Os^{III}-L-Co^{III} binuclear complexes with a number of peptide bridges as in [(NH₃)₅Os^{III}-L-Co^{III}(NH₃)₅](BF₄)₅, where L = iso(Pro)₀₋₄, iso(Phe)₂, iso(Gly)₂, iso = isonicotiny, have been synthesized and characterized. The peptide bridges are spacers that separate the Os^{III} center from the Co^{III} center. Upon one-electron reduction using pulse radiolysis techniques, the [(NH₃)₅Os^{II}-L-Co^{III}(NH₃)₅]⁴⁺ complexes are formed. These precursor complexes undergo intramolecular electron transfer on time scales varying from microseconds to many seconds. For L = iso(Pro)_n, n = 0-4, the rates of electron transfer, *k*_e (25 °C) (s⁻¹), and the activation parameters, Δ*H*[‡] (kcal/mol) and Δ*S*[‡] (eu), were, for n = 0, 1, 2, 3, 4, respectively, 1.9 × 10⁵, 10.2, 0; 2.7 × 10², 11.7, -8; 0.74, 12.7, -16; 0.9 × 10⁻¹, 12.4, -22; and 0.9 × 10⁻¹, 11.5, -25. For the more flexible iso(Gly)₂ and iso(Phe)₂ bridges, the rates of electron transfer, *k*_e (25 °C) (s⁻¹), and the activation parameters, Δ*H*[‡] (kcal/mol) and Δ*S*[‡] (eu), were 4.8, 11.4, -17; and 6.9, 12.2, -14, respectively. The Os(II) site in all of these complexes has approximately the same redox potential (-0.26 V vs. NHE). Because the driving force and reorganization energy in these complexes are very similar, variation in the rate of electron transfer can be related directly to the properties of the peptide bridge moiety. The rates of intramolecular electron transfer are more rapid than the rate of trans to cis proline isomerization, and therefore electron transfer takes place while the proline is in the extended trans configuration, the predominant isomer under these conditions.

Our earlier studies focused on metal to metal *intramolecular* electron-transfer reactions across amino acids, flexible and rigid polypeptides, and modified proteins.¹⁻³ Large changes in the rate of intramolecular electron transfer were observed when intervening peptide moieties were placed between a [(OH₂)(NH₃)₄Ru^{II}-] donor and an [(NH₃)₅Co^{III}-] acceptor in [(OH₂)(NH₃)₄Ru-L-Co(NH₃)₅] complexes (Ru-L-Co) (where L = iso(peptide), iso = isonicotiny). However, the Ru-L-Co complexes with varying peptide bridges exhibited *slow* rates of electron transfer (with time scales ranging from seconds to several days), and as a result, some of the differences between the peptide bridges were not observed.

In spite of the slow rates in the Ru-L-Co series, one important result of these studies with oligoproline bridges is that specific peptide motions, such as trans-cis proline isomerization, are important in controlling the distance between donor and acceptor, and thus in controlling the rate of electron transfer. Because proline isomerization is more rapid than electron transfer in the Ru-L-Co series,^{2,8,9} no quantitative information on the rate of electron transfer as a function of distance could be obtained in that series. This is especially true for the Ru-L-Co complexes with iso(Pro)₃ and iso(Pro)₄ bridges, where the measured rates were significantly *faster* than expected for iso(Pro)_n (n = 3, 4) bridges with extended all-trans conformations.

In order to study the effect of different peptide bridges and peptide motions on the rate of electron transfer, we have designed and synthesized a similar series of binuclear complexes where electron transfer takes place on a much faster time scale. The new compounds are a series of binuclear [(NH₃)₅Os-L-Co(NH₃)₅](BF₄)₅ complexes (where L = iso(peptide)) (Os-L-Co). In

this series oligoprolines and other flexible dipeptides are again used as bridging ligands, but [(NH₃)₅Os^{II}-] replaces [(OH₂)(NH₃)₄Ru^{II}-] as the electron donor. The use of the more strongly reducing Os(II) center significantly increases the rates of intramolecular electron transfer, so that electron transfer is much faster than the trans-cis proline isomerization. For these fast reactions in the Os-L-Co series, the question is whether intramolecular electron transfer will take place in the fully extended trans proline isomer or if it will occur only after trans-cis proline isomerization (*t*_{1/2} 1-2 min).^{8,9}

In this paper the synthesis and the intramolecular electron-transfer results for this new series of [(NH₃)₅Os-L-Co(NH₃)₅](BF₄)₅ (where L = iso(Pro)₀₋₄, iso(Phe)₂, and iso(Gly)₂) complexes are presented. A direct comparison between the osmium donors in this series and the ruthenium donors in the earlier study will be made. Also, the effect of changing the electron-transfer time scale on the trans-cis proline isomerization along the series will be discussed.

Experimental Section

Chemicals. L-Amino acids (99.9% pure) were purchased from Aldrich and Tridom Chemical Companies. Boc-amino acids were purchased from Bachem (Torrance, CA) and Peninsula Labs (San Carlos, CA). Solvents including DMF, CH₂Cl₂, THF, and ethyl acetate (EtOAc) were all glass-distilled and kept dry with molecular sieves. Other solvents (ethanol, ether) were reagent grade and were used as supplied. Trifluoroacetic acid (HTFA) (Aldrich) was used as supplied; trifluoromethanesulfonic acid (TFMS) (3 M) was glass-distilled before use. Dicyclohexylcarbodiimide (DCC) and hydroxybenzotriazole (HOBT) were purchased from Pierce and Tridom.

Resins, Packings, and HPLC Solvents. Pre-Pak 500-C₁₈ packing (37-50 μm) (Waters) was used for preparative reverse-phase chromatography. Ion-exchange resins Bio-Gel P-2 (200-400 mesh), Chelex 100 (100-200 mesh) (BioRad), and SP-Sephadex C-25 (Pharmacia) were used. HPLC grade methanol was purchased from JT Baker Co. HPLC solvents were filtered through Millipore membranes (Millipore Corp).

Preparations. I. Pentaamminecobalt Amino Acid and Peptide Complexes. The pentaamminecobalt amino acids and dipeptides were synthesized by the method of Isied et al.^{2,5} The [(NH₃)₅Os(TFMS)]-(TFMS)₂ was synthesized by literature methods.¹⁹

II. Preparation of Isonicotinic Acid Trifluoromethanesulfonate (A). To 4.0 g of isonicotinic acid (recrystallized from water) CF₃SO₃H (TFMS) was added dropwise with stirring until the isonicotinic acid dissolved. Then ethanol (≈10 mL) was added, followed by ethyl ether until turbidity began to appear. The resulting solution was cooled in ice to complete the precipitation. The solid was filtered, washed with ether, and dried over P₂O₅ in a vacuum desiccator overnight.

(1) Isied, Stephan S.; Vassilian, Asbed. *J. Am. Chem. Soc.* **1984**, *106*, 1726-1732.

(2) Isied, Stephan S.; Vassilian, Asbed. *J. Am. Chem. Soc.* **1984**, *106*, 1732-1736.

(3) Isied, Stephan S.; Kuehn, Christa; Worosila, Greg. *J. Am. Chem. Soc.* **1984**, *106*, 1722-1726.

(4) Isied, Stephan S. *Progr. Inorg. Chem.* **1984**, *32*, 443-557.

(5) (a) Rothe, M.; Theysohn, R.; Steffer, K. D.; Schneider, H.; Amani, M.; Kostrzewa, M. *Angew. Chem., Int. Ed. Engl.* **1970**, *8*, 919-20. (b) Rothe, M.; Rott, H. *Ibid.* **1970**, *15*, 770-1.

(6) (a) Chao, Y. H.; Bersohn, R. *Biopolymers* **1978**, *17*, 2761-7. (b) Chiu, H. C.; Bersohn, R. *Ibid.* **1977**, *16*, 277-288.

(7) (a) Grathwohl, C.; Wuthrich, K. *Biopolymers* **1978**, *17*, 2761-7. (b) Grathwohl, C.; Wuthrich, K. *Ibid.* **1976**, *15*, 2043-57.

(8) (a) Lin, L.; Brandt, J. F. *Biochemistry* **1983**, *22*, 553-9. (b) Brandt, J. F.; Halvorson, H. R.; Brennan, M. *Ibid.* **1975**, *14*, 4953.

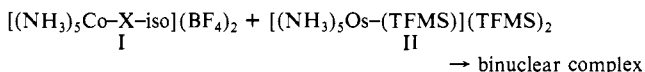
(9) Cheng, H. N.; Bovey, F. A. *Biopolymers* **1977**, *16*, 1465-72.

Table I. Elemental Analyses for $[(\text{NH}_3)_5\text{Co}-(\text{Pro})_n\text{-iso-Os}(\text{NH}_3)_5](\text{BF}_4)_5 \cdot x\text{H}_2\text{O}$ Complexes ($n = 0-4, x = 1-4$)

	$n = 0, x = 1$		$n = 1, x = 2$		$n = 2, x = 3$		$n = 3, x = 4$		$n = 4, x = 4$	
	calcd	obsd	calcd	obsd	calcd	obsd	calcd	obsd	calcd	obsd
C	7.25	7.33	11.92	11.61	15.70	15.53	18.83	18.65	21.47	20.71
H	3.65	3.50	4.09	3.96	4.45	4.24	4.74	4.91	4.99	4.62
N	15.51	15.61	15.16	14.87	14.88	14.29	14.65	14.58	14.45	14.23
Co			5.32	5.28	4.82	4.96				
Os			17.15	16.9	15.54	15.9				

III. Preparation of $[(\text{NH}_3)_5\text{Co-X-isonicotinyl}]^{3+}$ Where X = (Pro)_n ($n = 1, 2, 3, 4$), (GlyGly), or (PhePhe). Preparation was carried out by the method of Isied et al.²

IV. Synthesis of $[(\text{NH}_3)_5\text{Co-X-iso-Os}(\text{NH}_3)_5](\text{BF}_4)_5$ Binuclear Complexes Where X = (Pro)_n ($n = 0, 1, 2, 3, 4$), (GlyGly), (PhePhe), and iso = Isonicotinyl. The general reaction for all of these syntheses was



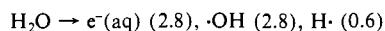
In each case the deprotonated cobalt complexes (I) were generated by dissolving the corresponding protonated complex in about 1 mL of water, adding a drop of N-Methylmorpholine, and precipitating the complex by adding ethanol and ether. The complexes were washed with ether and dried in a vacuum desiccator.

The binuclear complexes were then synthesized as follows: 0.1 mmol of I was added to a solution of II (0.15 mmol)¹⁹ in dry acetone (200 μL). The solution was stirred at room temperature for 8–12 h. The initial suspension slowly dissolved resulting in a brown orange solution. This solution was then diluted with 0.3 M trifluoroacetic acid (HTFA), applied onto a small (6 cm \times 1.5 cm) SP-Sephadex C-25 column, and eluted with 0.3 M HTFA. After the unreacted starting materials were eluted with 0.3 M HTFA, the binuclear complex was eluted with 1.0 M HTFA as a pink orange solution. The solution was concentrated by rotary evaporation. The BF_4^- salt was precipitated by addition of 0.5 mL of HBF_4 , one volume of ethanol, and two volumes of ether. The precipitate was collected, washed with ether, redissolved in 1 mL of water, and applied to a Bio-Gel P-2 column (200–400 mesh, 40 cm \times 1 cm). The main band was collected and concentrated to dryness by rotary evaporation, resulting in a shiny pink-orange solid. The final yields for the complexes isolated varied between 25 and 47%.

V. Methods. HPLC was carried out on a Waters Associates liquid chromatography system equipped with both a variable wavelength UV detector and a fixed wavelength detector, in order to monitor at two different wavelengths simultaneously, when needed. A solvent system containing water/methanol with up to 0.2% HTFA was used for the elution of cobalt complexes of the hydrophobic peptides. Two types of high-pressure columns were used: Altex C₁₈ columns (5 μm , 4.6 mm \times 25 cm) and Waters Radial Pak C₁₈ columns (10 μm , 8 mm \times 10 cm). With the radial pak columns a Waters Radial Compression Module (Model RCM 100) was used. Preparative scale columns were used to isolate the peptide complexes as described earlier.¹⁰

Differential pulse polarography measurements were done in 0.1 M HTFA using a PAR Model 174A polarographic analyzer, and cyclic voltammograms were recorded with a PAR Model 173 potentiostat, a Model 175 universal programmer, and an Omnigraph 2000 X-Y recorder. A three-electrode cell with a glassy carbon electrode, a standard calomel reference electrode, and a platinum wire auxiliary electrode was used.

Kinetics Experiments: Intramolecular Reactions. The kinetics of intramolecular electron transfer in the Os–L–Co complexes were determined by using pulse radiolysis techniques. In the pulse radiolysis, irradiated water forms the following species:^{11,12}



The numbers in parentheses denote *G* values, the number of radicals formed per 100 eV absorbed. Reducing radicals, $\text{CO}_2^{\cdot-}$ and $(\text{CH}_3)_2\text{COH}\cdot$, were produced from the $\cdot\text{OH}$ radicals by hydrogen atom abstraction from

Table II. Reduction Potentials of the $[(\text{NH}_3)_5\text{Os}^{\text{III}}\text{-iso}(\text{Pro})_n]$ Series

n	$E_{1/2} \text{ Os}^{\text{III/II}}, \text{ V vs. NHE}$
0	-0.23
1	-0.27
2	-0.27
3	-0.25
4	-0.26

the corresponding molecules. The $\cdot\text{OH}$ and $\cdot\text{H}$ radicals also decay by dimerization and cross reaction.

Experiments were carried out at radical precursor concentrations of 0.1 M sodium formate and 0.1 M 2-propanol.

Solutions of the $\text{Os}^{\text{III}}\text{-L-Co}^{\text{III}}$ binuclear complexes (ca. 1×10^{-4} – 1×10^{-5} M) were prepared immediately before use by dissolving the appropriate weight of the complex in 50 mL of a solution of 0.1 M HTFA and 0.1 M 2-propanol. The solutions were degassed for 30 min and transferred under argon pressure to a 2-cm cell (2 cm \times 1 cm \times 0.5 cm). The analyzing light, produced by a quartz iodine lamp with a filter cutoff below 450 nm, passed through the cell 3 times, resulting in a path length of 6.1 cm. Pulses of 0.5–1- μs duration were used (Van de Graaf accelerator, Brookhaven National Laboratory, 2 MeV) to produce radical concentrations between 5×10^{-7} and 5×10^{-6} M. For the Os–iso–Co complex, experiments were done with a 10^{-3} M complex using $\text{CO}_2^{\cdot-}$ radical. This was necessary because the $\text{Os}^{\text{III}}\text{-iso-Co}^{\text{III}}$ intermediate in this case decays rapidly (see Results).

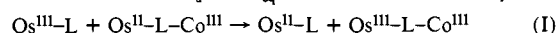
Intermolecular Reactions. Freshly prepared solutions of $[(\text{NH}_3)_5\text{Co}-(\text{Pro})]^{3+}$ (5×10^{-3} M) were degassed in a spectrophotometric cell and added to a known amount of $[(\text{NH}_3)_5\text{Os}^{\text{III}}\text{-iso}]^{3+}$. The electron-transfer reaction was initiated by the addition of a known amount of Eu^{2+} to the reaction mixture. This generated a specific amount of $\text{Os}(\text{II})$, and the rate of the oxidation of the $\text{Os}(\text{II})$ complex was monitored at $\lambda = 525$ nm.

Treatment of the Data. Transients were detected spectrophotometrically (at 525 nm) as described in ref 13. Spectra of the intermediates were obtained by varying the wavelength between 400 and 600 nm.

The intermediate precursor complex was formed by successive generation of known radical concentrations, such that the total radical $\text{CO}_2^{\cdot-}$ generated did not exceed 5% of the $\text{Os}^{\text{III}}\text{-L-Co}^{\text{III}}$ reactant. The unimolecular rate of electron transfer was calculated directly from the $\ln A$ vs. t plot and was corrected for the presence of $\text{Os}(\text{III})$ product using

$$k_{\text{obsd}} = k_u / (1 + [\text{Os}^{\text{III}}\text{L}] / [\text{Os}^{\text{III}}\text{L-Co}^{\text{III}}] K_{\text{eq}})$$

where k_u is the unimolecular rate constant and K_{eq} is the equilibrium constant for reaction I. The k_u and K_{eq} were determined from a plot of



$1/k_{\text{obsd}}$ vs. $[\text{Os}^{\text{III}}\text{L}] / [\text{Os}^{\text{III}}\text{LCo}^{\text{III}}]$.

Results

Synthesis and Characterization of the Complexes. The binuclear $[(\text{NH}_3)_5\text{Os-L-Co}(\text{NH}_3)_5](\text{BF}_4)_4$ complexes, where L = iso(Pro)_n, $n = 0-4$, iso(Gly)₂, or iso(Phe)₂, were synthesized by adding the $[(\text{NH}_3)_5\text{Co}^{\text{III}}\text{Xiso}]^{2+}$ complexes (X = amino acid or peptide) to the $[(\text{NH}_3)_5\text{Os}(\text{TFMS})]^{2+}$ in dry acetone. After chromatographic purification, the complexes were characterized by a number of physicochemical techniques. Elemental analyses of the complexes (C,H,N,Co,Os) are summarized in Table I. The elution behaviors

(10) Isied, Stephan S.; Vassilian, Asbed; Lyon, John M. *J. Am. Chem. Soc.* **1982**, *104*, 3910–3916.

(11) (a) Ross, A. B. "Selected Rates of Reaction of Transients from Water in Aqueous Solution, Hydrated Electron, Supplemental Data". *Natl. Stand. Ref. Data Ser. (U.S., Natl. Bur. Stand.)* **1975**, NSRDS-NBS-43 Supplement. (b) Dorfman, L. M.; Adams, G. E. "Reactivity of the Hydroxyl Radical in Aqueous Solution". *Natl. Stand. Ref. Data Ser. (U.S., Natl. Bur. Stand.)* **1973**, NSRDS-NBS-4 Report.

(12) Van Leeuwen, J.; Raap, A.; Koppenol, W.; Nauta, H. *Biochim. Biophys. Acta* **1978**, *503*, 1–9 and references therein.

(13) Schwarz, H. A.; Creutz, C. *Inorg. Chem.* **1983**, *22*, 707–13.

(14) Sutin, N. *Acc. Chem. Res.* **1982**, *15*, 275–282.

(15) (a) Hoffman, M. Z.; Simic, M. *J. Am. Chem. Soc.* **1972**, *94*, 1757.

(b) Hoffman, M. Z.; Simic, M. *J. Am. Chem. Soc.* **1970**, *92*, 5533. (c) Hoffman, M. Z.; Simic, M. G.; Breznjak, N. V.; Whitburn, K. D. *Inorg. Chem.* **1980**, *19*, 3180.

(16) The $\text{CO}_2^{\cdot-}$ was produced in 10 to 30 small pulses separated by 0.05 s to minimize radical–radical reactions in competition with reaction 2. Also, the value of the rate constant was calculated from the appropriate equation for decay with reactant in equilibrium with product with $K_{\text{eq}} = 1$.

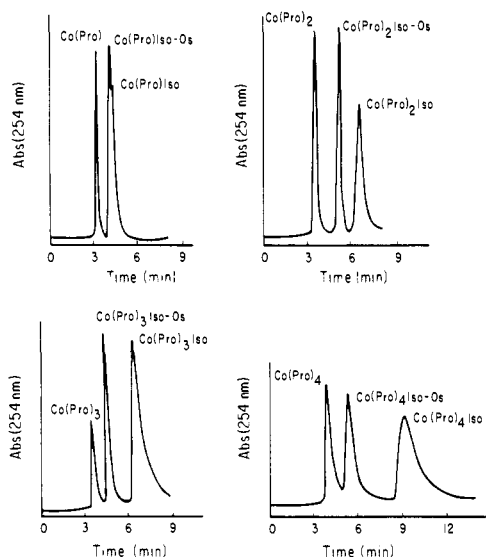


Figure 1. HPLC elution profiles of synthetic mixtures of $[(\text{NH}_3)_5\text{Co}(\text{Pro})_n]^{3+}$, $[(\text{NH}_3)_5\text{Co}(\text{Pro})_n\text{iso}]^{3+}$, and $[(\text{NH}_3)_5\text{Co}(\text{Pro})_n\text{iso-Os}(\text{NH}_3)_5]^{5+}$ for $n = 1-4$. Conditions: C_{18} column (10 cm \times 0.8 cm), 5 μm ; 20% $\text{CH}_3\text{OH}/\text{H}_2\text{O}$, 0.1% HTFA, pH 2.65 (adjusted with NaOH), flow 1 mL/min; $\lambda = 254$ nm.

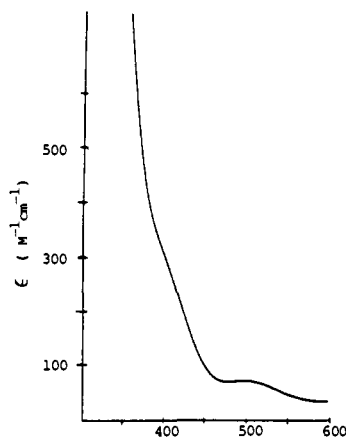
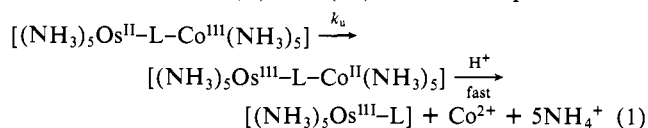


Figure 2. UV-vis spectrum of $[(\text{NH}_3)_5\text{Os-L-Co}(\text{NH}_3)_5]^{5+}$, L = iso(Pro), in 0.1 M HTFA.

of the cobalt peptide complexes^{1,10} and the Os-L-Co (L = iso(peptide)) complexes were also used as a criterion of purity. Figure 1 summarizes the elution profile for the Os-L-Co complexes (prior to electron transfer) and the corresponding Co(III) products of the reaction. The visible spectra of all the Os-L-Co complexes are similar. A representative spectrum, that of $[(\text{NH}_3)_5\text{Os-iso-Pro-Co}(\text{NH}_3)_5]^{5+}$ in 0.1 M HTFA is given in Figure 2. The shoulder at 500 nm corresponds to the d-d transitions of the Co(III) site overlapping with the more intense Os(III) charge-transfer transitions. The reduction potentials of the Os(III) center in these complexes were determined by cyclic voltammetry and differential pulse polarography of the osmium peptide complexes after the removal of the cobalt center. Table II summarizes the results of the electrochemical measurements. The circular dichroism (CD) spectra in the UV region of the $[(\text{NH}_3)_5\text{Co}(\text{Pro})_n]^{3+}$ ($n = 3, 4$) complexes are shown in Figure 3.

Kinetics of Electron Transfer. The intramolecular electron-transfer reaction studied in this series, where an electron is transferred from an Os(II) to Co(III), is shown in eq 1. Titration



of the parent Os(III) complexes with Eu^{2+} verified that the reductions are quantitative in 0.1 M HTFA and allowed the Os(III)

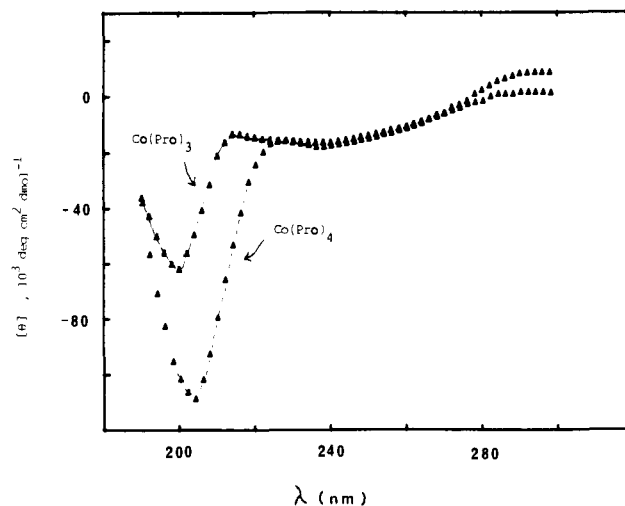


Figure 3. CD spectra of $[(\text{NH}_3)_5\text{Co}(\text{Pro})_n]^{3+}$ ($n = 3, 4$) complexes in 0.1 M HTFA.

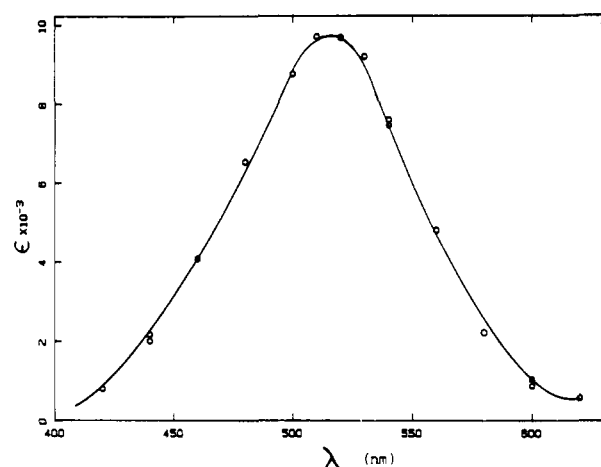


Figure 4. Spectrum of the $[(\text{NH}_3)_5\text{Os}^{\text{II}}\text{-L-Co}^{\text{III}}(\text{NH}_3)_5]^{5+}$, L = iso, intermediate generated by pulse radiolysis.

products to be characterized by HPLC, visible spectra, and electrochemical measurements.

In the pulse radiolysis experiments the Os(II) complexes were produced by the rapid reduction of the parent Os(III) complexes with $(\text{CH}_3)_2\text{C}\dot{\text{O}}\text{H}$ or $\text{CO}_2^{\cdot-}$ (eq 2). The generation and subsequent

$$[(\text{NH}_3)_5\text{Os}^{\text{III}}\text{-L-Co}^{\text{III}}(\text{NH}_3)_5] + (\text{CH}_3)_2\text{C}\dot{\text{O}}\text{H} \rightarrow [(\text{NH}_3)_5\text{Os}^{\text{II}}\text{-L-Co}^{\text{III}}(\text{NH}_3)_5] + (\text{CH}_3)_2\text{CO} + \text{H}^+ \quad (2)$$

decay of the Os(II) was followed at 525 nm. Spectra are similar for all Os(II) complexes studied, and a typical spectrum is shown in Figure 4. This spectrum is very similar to that of many $[(\text{NH}_3)_5\text{Os}^{\text{II}}\text{-pyridine}]$ complexes.¹⁷ Rate constants for reaction 2 at 25 $^\circ\text{C}$ are all about $6 \times 10^8 \text{ M}^{-1} \text{ s}^{-1}$. Rate constants for the reduction by $\text{CO}_2^{\cdot-}$ radical are larger (i.e., $4 \times 10^9 \text{ M}^{-1} \text{ s}^{-1}$ for the L = iso(Pro)₃ complex).

$[(\text{NH}_3)_5\text{Os-iso-Co}(\text{NH}_3)_5](\text{BF}_4)_5$. For the Os^{III}-iso-Co^{III} complex, in a $1 \times 10^{-4} \text{ M}$ solution containing 0.1 M formate and HTFA (pH \sim 2), growth of Os^{II}-iso-Co^{III} occurred at $4 \times 10^5 \text{ s}^{-1}$ and the subsequent decay gave $k_u = 1.9 \times 10^5 \text{ s}^{-1}$ at 25 $^\circ\text{C}$. An increase in the Os^{III}-iso-Co^{III} concentration to $3 \times 10^{-3} \text{ M}$ caused a corresponding increase in growth rate, but the decay was

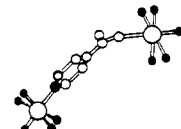
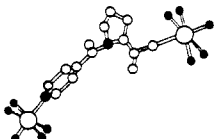
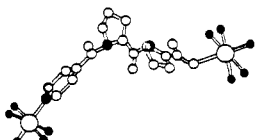
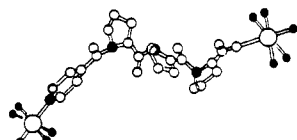
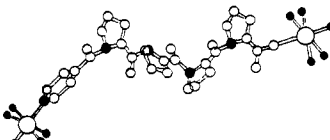
(17) Sen, J.; Taube, H. *Acta Chem. Scand. Ser. A* 1979, A33(2), 125-135.

(18) For $n = 3$ and 4 prolines, the intramolecular electron-transfer rate constant reported is that measured in the presence of excess Os^{III}-L-Co^{III}. Under these conditions the rate measured is an upper limit (see Discussion).

(19) Lay, P.; Magnuson, R.; Sen, J.; Taube, H. *J. Am. Chem. Soc.* 1982, 104, 7658.

(20) For the Os-L-Co complexes (L = iso(Pro)_n, $n = 0-4$), the error limit in the rate constants for $n = 0, 1, 2$ is $\pm 4\%$. For $n = 3, 4$, the error limit is $\pm 8\%$. For $n = 0, 1, 2$, $\Delta H^\ddagger = \pm 0.5 \text{ kcal/mol}$. For $n = 3, 4$, $\Delta H^\ddagger = \pm 1 \text{ kcal/mol}$.

Table III. Intramolecular Electron-Transfer Rates and Activation Parameters for the $[(\text{NH}_3)_5\text{Os}^{\text{II}}\text{-iso}(\text{Pro})_n\text{-Co}^{\text{III}}(\text{NH}_3)_5]^{4+}$, $n = 0-4$, Series^a

	k_u (25 °C)	ΔH^\ddagger , kcal/mol	ΔS^\ddagger , eu
	1.9×10^5	10.2	0
	2.7×10^2	11.7	-8
	0.74	12.7	-16
	$0.9 \times 10^{-1}{}^b$	12.4	-22
	$0.9 \times 10^{-1}{}^b$	11.5	-25

^a Reference 20. ^b Reference 18.

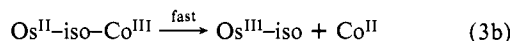
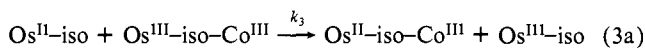
Table IV. Electron-Transfer Rate Constants (k , s^{-1}) for the $[(\text{NH}_3)_5\text{Os}^{\text{II}}\text{-L-Co}^{\text{III}}(\text{NH}_3)_5]^{4+}$ Series^a

	L				
	iso	iso(Pro) ₁	iso(Pro) ₂	iso(Pro) ₃	iso(Pro) ₄
	0.75×10^5 (10)	53 (5)	0.35 (15)	0.09 (25)	0.09 (25)
	1.9×10^5 (25)	120 (15)	0.74 (25)	0.24 (40)	0.27 (41)
	5.7×10^5 (41.5)	270 (25)	2.4 (41)	0.73 (55)	0.32 (45)
	8×10^5 (51)	1520 (54)	3.3 (47)	0.84 (60)	0.59 (55)
			5.8 (54)		

^a Temperature (°C) in parentheses.

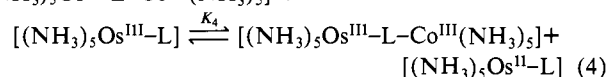
essentially the same, $2.1 \times 10^5 \text{ s}^{-1}$ (Figure 5a). The rate constants and activation parameters obtained in 10^{-4} M solution are given in Tables III and IV.

Osmium Electron-Exchange Reactions. The rate of electron exchange between Os(II) and Os(III) complexes was measured using $\text{Os}^{\text{II}}\text{-iso-Co}^{\text{III}}$, which rapidly decays as shown in eq 3. A



$5 \times 10^{-4} \text{ M}$ solution of $[(\text{NH}_3)_5\text{Os}^{\text{III}}\text{-iso}]$ containing 5×10^{-5} to $3 \times 10^{-4} \text{ M}$ $[(\text{NH}_3)_5\text{Os}^{\text{III}}\text{-iso-Co}^{\text{III}}(\text{NH}_3)_5]$ was partially reduced by generating $\text{CO}_2^{\cdot-}$. Since $[\text{Os}^{\text{III}}\text{-iso}]$ was in excess, $[\text{Os}^{\text{II}}\text{-iso}]$ is the principal product of the reduction, and rate constant k_3 was found to be $5 \times 10^5 \text{ M}^{-1} \text{ s}^{-1}$.

Because reaction 3 is a special case of the general electron-exchange reaction (eq 4), which is close to thermoneutral for all $[(\text{NH}_3)_5\text{Os}^{\text{II}}\text{-L-Co}^{\text{III}}(\text{NH}_3)_5] +$



the proline ligands ($K_4 = 1$), k_4 (and k_{-4}) should be nearly the same as k_3 , $5 \times 10^5 \text{ M}^{-1} \text{ s}^{-1}$. Since the $\text{Os}^{\text{III}}\text{-L}$ complex is a product of reaction 1, reaction 4 acts to retard the overall decay of Os(II) when large pulses or many small pulses are given to the sample.

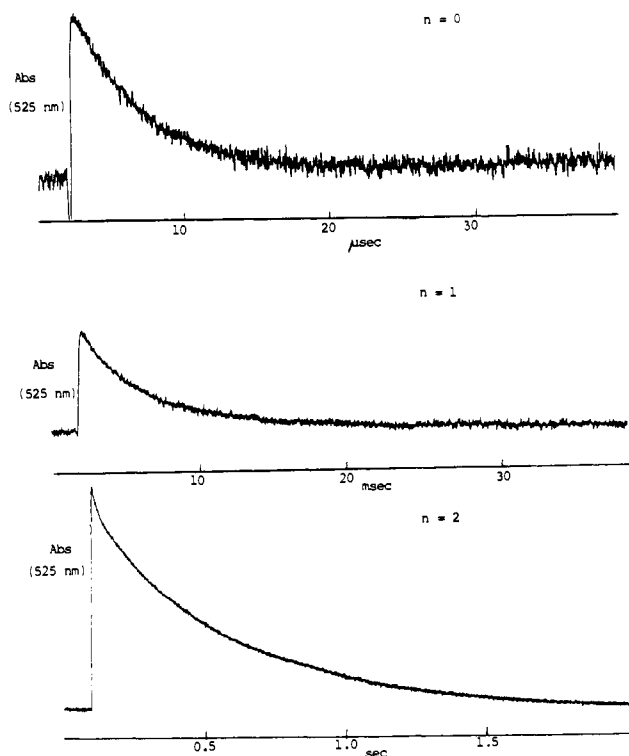
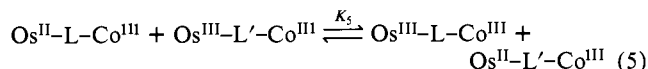


Figure 5. Intramolecular electron-transfer rates in $[(\text{NH}_3)_5\text{Os}^{\text{III}}\text{-L-Co}^{\text{III}}(\text{NH}_3)_5]^{5+}$, $L = \text{iso}(\text{Pro})_n$, $n = 0$ (a, top), 1 (b, center), 2 (c, bottom), by $\text{CO}_2^{\cdot-}$ radical on the microseconds, milliseconds, and seconds time scale. Experiments a and b are at 25 °C, c is at 41 °C.

Although the experimental conditions used favor the extended trans proline isomers, the presence of small amounts of other proline isomers can affect the kinetics of intramolecular electron transfer (eq 5, where L is a fully trans-extended proline oligomer and L' is the same proline oligomer, but with one or more cis



linkages). For eq 5, the k_5 is expected to be similar to k_4 , or $5 \times 10^5 \text{ M}^{-1} \text{ s}^{-1}$, and the equilibrium constant K_5 should be 1. Reaction 5 is important as it can provide a rapid mechanism for cis-trans equilibration as long as the L' complex is at a higher concentration than the Os(II) produced (typically $5 \times 10^{-7} \text{ M}$).

[(NH₃)₅Os^{III}-L-Co^{III}(NH₃)₅] Where L = iso(Pro)_n, n = 1-4. For Os^{III}-L-Co^{III} complexes, where L = iso(Pro)_n, n = 1-4, the intramolecular electron-transfer reaction (eq 1) is slow enough so that low concentration of the parent Os^{III}-L-Co^{III} could be used and still maintain reaction 2 much faster than reaction 1. The concentration of Os^{III}-L-Co^{III} commonly used was $2 \times 10^{-5} \text{ M}$, so the [Os(II)] grew at a rate of 10^4 s^{-1} , or at least 20 times the decay rate (Figure 5b,c). Rate constants and activation parameters are given in Tables III and IV for solutions of complexes with one to four bridging prolines in which about $5 \times 10^{-7} \text{ M}$ Os^{II}-L-Co^{III} was generated.

For Os^{III}-isoPro-Co^{III}, the approach to equilibrium (eq 4-5) is slow compared to the rate of intramolecular electron transfer and is equal to $k_4[\text{Os}^{\text{III}}]_{\text{total}}$, or 10 s^{-1} in $2 \times 10^{-5} \text{ M}$ solutions. The decay of [Os^{II}-isoPro-Co^{III}] is sufficiently rapid (270 s^{-1} at 25°C) so that the effect of reactions 4 and 5 is not observed. For example, no effect of multiple pulsing the sample, up to 30% consumption of the starting materials, was seen at 25°C and above, but the apparent rate constant did decrease with increasing number of pulses at 5°C , where $k_{\text{a}} = 53 \text{ s}^{-1}$.

For Os^{III}-iso(Pro)_n-Co^{III} (n = 2, 3, 4), reactions 4 and 5 (if any) should be at equilibrium during the decay of the Os^{II}-L-Co^{III} complexes. The observed rate constant should decrease with increasing number of pulses given to the sample because of the accumulation of the Os^{III}-L product. The observed rate constant when $K_4 = 1$ is

$$k_{\text{obsd}} = \frac{k_{\text{a}}}{1 + \frac{[\text{Os}^{\text{II}}-\text{L}]}{[\text{Os}^{\text{III}}-\text{L}-\text{Co}^{\text{III}}]}} \quad (6)$$

For the complex with n = 2, eq 6 fits the observed rate data well up to 30% depletion.

For the L = iso(Pro)_n (n = 3, 4) complexes, the kinetics of intramolecular electron transfer were studied under two sets of conditions: with and without excess Os^{III}-L-Co^{III} present. In the first set of conditions the Os^{III}-L-Co^{III} was always in excess because $2 \times 10^{-5} \text{ M}$ complex was used, and only $5 \times 10^{-7} \text{ M}$ Os^{II}-L-Co^{III} was generated. Under these conditions eq 5 applied. The result under these conditions for the complex with n = 3 was that the decay of Os(II) deviated noticeably from first order, being somewhat more rapid in the early part of the decay than in the later part. For n = 4, the effect was more pronounced, and an exponential and a linear term in time were used to fit the data. The observed rate constant for n = 4 is perhaps most accurate for the first half-life. For these experiments (n = 3, 4), values of k_{a} were calculated for about 5-10 pulses. The apparent k_{a} decreased by about 50% on the first few pulses, then remained constant when the ratio, $[\text{Os}^{\text{III}}-\text{L}]/[\text{Os}^{\text{III}}-\text{L}-\text{Co}^{\text{III}}]$, was between 0.1 and 0.3. The data in Table IV are averages for this region. (The origin of the large rates for the first few pulses is unknown, but may be due to a 10^{-6} M impurity. This impurity would be negligible for the faster reacting complexes, n = 0, 1, 2.)

In the other study on the L = iso(Pro)_n, n = 3, 4 complexes, the major portion of the complexes was reduced under conditions where eq 5 cannot operate to equilibrate the sample. When 30-90% of the complex was reduced,¹⁷ the rate constant for the disappearance of the precursor complex changed from 0.09 s^{-1} to 0.04 s^{-1} for n = 3 and from 0.09 s^{-1} to 0.01 s^{-1} for n = 4.

Note that the rates and activation parameters given in Table III are those obtained under conditions of excess Os^{III}-L-Co^{III} for all the complexes studied (n = 0-4). In Figure 6 the rates are plotted vs. n, including for n = 3 and 4, the rates in the presence and absence of large amounts of Os^{III}-L-Co^{III}.

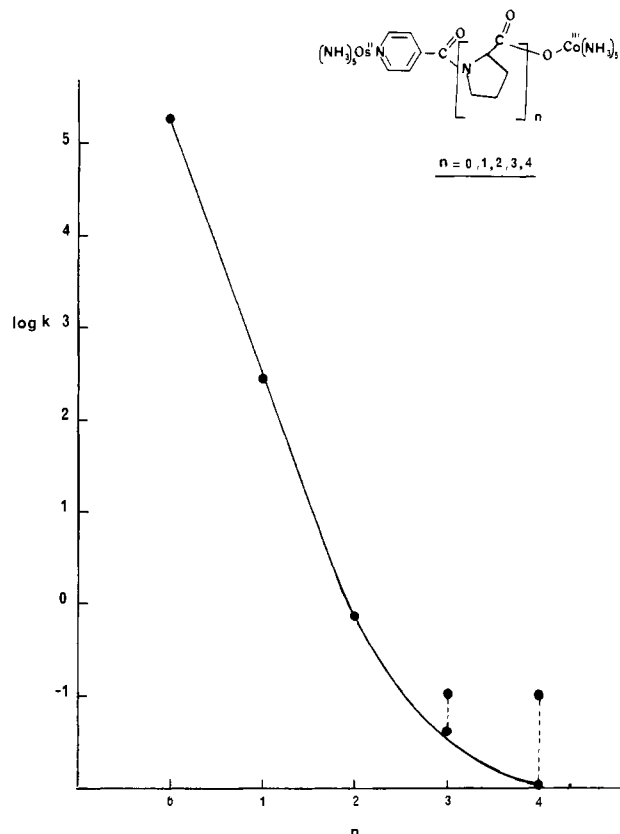


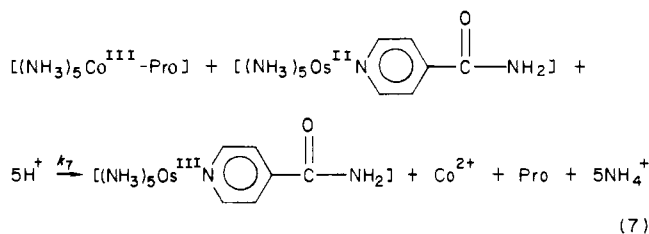
Figure 6. Plot of log k , the rate constant for intramolecular electron transfer, vs. the number of proline residues in the series [(NH₃)₅Os^{II}-L-Co^{III}(NH₃)₅], L = iso(Pro)_n, n = 0-4. The upper points for n = 3, 4 represent the enhanced rates due to equilibration of different conformers. (See Results.)

Table V. Electron-Transfer Rate Constants vs. Temperature for [(NH₃)₅Os-L-Co(NH₃)₅]⁵⁺ Complexes

L = iso(Gly) ₂		L = iso(Phe) ₂		L = iso(Pro) ₂	
k_{a} , s ⁻¹	T, °C	k_{a} , s ⁻¹	T, °C	k_1 , s ⁻¹	T, °C
1.8	11	3.5	15.5	0.74	25
4.8	25	6.9	25	2.4	41
12.8	41	27.8	45	5.8	54
32.5	56				

Flexible Dipeptide Complexes. The [(NH₃)₅Os-L-Co(NH₃)₅]⁵⁺ complexes, where L = iso(Gly)₂ and iso(Phe)₂, were studied under similar conditions to those used for the L = iso(Pro)₂ analogue. Table V summarizes the rate constants for these complexes at different temperatures. By use of these rates, ΔH^\ddagger and ΔS^\ddagger values of 11.4 kcal/mol, -17 eu, and 12.2 kcal/mol, -14 eu, were calculated for the L = iso(Gly)₂ and iso(Phe)₂ complexes, respectively.

Intermolecular Electron Transfer between Co(III) and Os(II) Complexes. In order to estimate the possible interference from the intermolecular reaction between the Os(II) complex and the Co(III)-peptide complex, the rate of the following second-order reaction was studied.



The k_7 is calculated to be $k_7 = 28 \text{ M}^{-1} \text{ s}^{-1}$, with $\Delta H^\ddagger = 10.8 \pm 0.2 \text{ kcal/mol}$ and $\Delta S^\ddagger = 15 \pm 1 \text{ eu}$.

Discussion

Oligoproline Complexes. In this paper and other papers in this series intramolecular electron-transfer reactions are studied as the bridging group changes between a metal donor and a metal acceptor.¹⁻⁴ Because the reactions described here are rapid, pulse radiolysis provides a convenient way to generate the precursor complex and measure the rate. This technique has been used earlier by Hoffman et al. for the measurement of rates of intramolecular electron transfer in a series of (*p*-nitrobenzoato)-pentaamminecobalt(III) complexes.¹⁵

In this paper we report on the first series of [(NH₃)₅Os^{III}-L-Co^{III}(NH₃)₅](BF₄)₅ binuclear complexes. These complexes where L = iso(Pro)_{*n*}, *n* = 0-4, were synthesized by the reaction of [(NH₃)₅Co^{III}-L] (with the carboxylate end of L attached to Co) with [(NH₃)₅Os(TFMS)](TFMS)₂ in acetone. Ion-exchange and reverse-phase HPLC were used for identification and separation of the complexes. In comparison to the analogous Ru^{III}-L-Co^{III} complexes,^{1,2} the Os^{III}-L-Co^{III} complexes are more susceptible to attack by base, resulting in the slow formation of OsO₂, and therefore all manipulations of these complexes were carried out in weakly acidic media.

The Os-L-Co complexes, L = iso(Pro)_{*n*}, exist predominantly in the trans proline configuration under the experimental conditions. Earlier NMR and CD studies of oligoproline peptides showed that the fully extended trans isomer predominates in aqueous acidic media.⁵⁻⁷ The pronounced CD effect observed for the [(NH₃)₅Co(Pro)_{*n*}]²⁺ (*n* = 3, 4) complexes (Figure 3) is an indication of the onset of a peptide secondary structure in these oligoproline complexes. The half-life for proline isomerization (trans to cis) is also known to be 1-2 min.^{8,9} Therefore, except for the Os-L-Co complexes where L = iso(Pro)_{*n*}, *n* = 3, 4, the intramolecular rates of electron transfer are faster than the rate of proline isomerization.

In the Os-L-Co complexes, where L = iso(Pro)_{*n*}, *n* = 0-2, the rate constant for intramolecular electron transfer decreases by about a factor of 500 per proline. The rates decrease with distance exponentially as in eq 8. For $\Delta r = 3.1 \text{ \AA}$, which is the distance

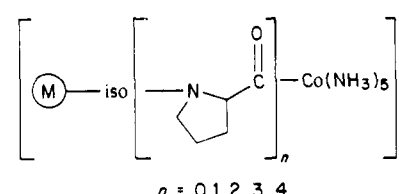
$$k_u = k_0 e^{-\beta \Delta r} \quad (8)$$

between proline residues in trans polyproline, β equals 2.0 \AA^{-1} . This is in the expected range of β (1.4-2.0 \AA^{-1}), calculated for other systems.¹⁴

As the rate of electron transfer decreases for L = iso(Pro)_{*n*}, *n* = 3, 4, the possibility for equilibration between different forms of trans-cis isomers begins to interfere with the observed rate of electron transfer. Therefore these two complexes were investigated under two different conditions. In the first case, $2 \times 10^{-5} \text{ M}$ [Os^{III}-L-Co^{III}] solutions were used, and $5 \times 10^{-7} \text{ M}$ [Os^{II}-L-Co^{III}] was generated; thus a large excess of [Os^{III}-L-Co^{III}] remained to maintain equilibrium with the [Os^{II}-L-Co^{III}] formed during the electron-transfer process. Under these conditions a rate constant of 0.09 s⁻¹ was observed for *n* = 3 and *n* = 4. Under different conditions, when most of the [Os^{III}-L-Co^{III}] is reduced to [Os^{II}-L-Co^{III}], the rate constants for *n* = 3 and 4 decreased to 0.04 s⁻¹ and 0.01 s⁻¹, respectively. Thus, a range of rates, 0.09-0.04 s⁻¹ for *n* = 3 and 0.09-0.01 s⁻¹ for *n* = 4, represents rates for different proline conformers, with varying distances between the metal centers.

A plot of rate constants vs. the number of bridging proline residues in Os^{III}-L-Co^{III} complexes is shown in Figure 6. For *n* = 3 and 4, the range of rates obtained under two different experimental conditions is plotted. The lower rate constants for *n* = 3 and 4 are more realistic approximations for the *k* vs. *n* plot, since no interference from Os^{III}-L-Co^{III} is possible. The leveling off for *n* = 3 and 4 prolines may be due to the presence of proline conformers where the two metals are at closer distances than in the predominant all-trans isomer of the time scale of the electron-transfer process.

Table VI. Intramolecular Electron Transfer across Oligoprolines



<i>n</i>	complex ^a	<i>k</i> _{Ru} , s ⁻¹	<i>k</i> _{Os} , s ⁻¹
0	Co-iso-(M)	1.2×10^{-2}	1.9×10^5
1	Co-Pro-iso-(M)	1.0×10^{-4}	2.7×10^2
2	Co-(Pro) ₂ iso-(M)	0.64×10^{-5}	0.74
3	Co-(Pro) ₃ iso-(M)	5.6×10^{-5}	0.9×10^{-1b}
4	Co-(Pro) ₄ iso-(M)	14.0×10^{-5}	0.9×10^{-1b}

^a M = SO₄(NH₃)₄Ru- or (NH₃)₅Os- at 25 °C. ^b Reference 18.

The temperature dependence for the rate of intramolecular electron transfer in the [Os-L-Co], L = iso(Pro)_{*n*}, *n* = 0-2, series, correlates well with an increase in the distance between the two metal centers (Tables III and IV). A slight increase in ΔH^\ddagger from 10.2 to 12.7 kcal/mol can be attributed to the 1/*r* distance dependence of the outer sphere reorganization energy for the precursor complexes.

The decrease in the electronic matrix coupling element (β) is seen as an increasingly more negative ΔS^\ddagger along the series. For L = iso(Pro)_{*n*}, *n* = 3, 4 prolines, the rates and activation parameters reflect a range of different conformers undergoing electron transfer on the same time scale as trans to cis proline isomerization. The rates and activation parameters for *n* = 3, 4 prolines (Tables III and IV) are probably due to composite processes, and are reported only for comparison with those for the *n* = 0-2 cases.

Flexible Dipeptide Complexes. In addition to the series with oligoproline bridging ligands, two other complexes with flexible dipeptide bridging ligands were studied under identical conditions. In Table V the three complexes, [(NH₃)₅Os-L-Co(NH₃)₅]⁵⁺, where L = iso(Gly)₂, iso(Phe)₂, and iso(Pro)₂, have the same number of bridging atoms between the metal centers with differences only in the structure and conformation of the amino acid side chains. The flexible dipeptide complexes with L = iso(Gly)₂ or iso(Phe)₂ undergo intramolecular electron transfer 5-10 times faster than the rigid dipeptide complex with L = iso(Pro)₂. Although the difference is small, these faster rates may be a reflection of a closer approach between the donor and acceptor in the flexible dipeptide bridges than in the rigid analogue. This small rate increase further indicates that the average distance between the donor and acceptor does not change significantly in this series of bridging dipeptides. However, the rates for these three complexes with dipeptide bridges are still much slower than that for the analogous complex with only one proline separating the metal centers.

Comparisons between the [Os^{II}-L-Co^{III}] and the Corresponding [Ru^{II}-L-Co^{III}] Series Where L = iso(Pro)_{*n*}, *n* = 0, 1, 2, 3, 4. A more detailed understanding of the rates of intramolecular electron transfer in the Os-L-Co series can be obtained by comparison with the corresponding Ru-L-Co series. In Table VI we present the most extensive comparison between two electron-transfer series where the main difference is in the driving force of the reaction.

The use of Os-L-Co, instead of Ru-L-Co peptide complexes has increased the driving force of the reaction by more than 600 mV. As a result of the increase in driving force, substantial increase in the rate of intramolecular electron transfer is observed for the Os-L-Co series over the Ru-L-Co series. The reaction time scales for the Os-L-Co series varied from microseconds to seconds, whereas for the corresponding Ru-L-Co complexes, from seconds to days.

The Os-L-Co series showed a more significant drop in rate than the Ru-L-Co series for L = iso(Pro)_{*n*}, *n* = 0-2. Furthermore, the Ru-L-Co series for L = iso(Pro)_{*n*}, *n* = 3, 4, showed an increase in rate over that for *n* = 2. This unexpected increase in rate was attributed to trans to cis proline isomerization (*t*_{1/2} = 1-2 min),^{8,9}

which reduces the distance between the ruthenium and cobalt centers.² The corresponding Os-L-Co series (L = iso(Pro)_n) showed a decrease in rate, although lower than expected, in going from $n = 2$ to $n = 3$ (Table VI).

The range of rate constants for the Os-L-Co series (factor of 10⁷) is much greater than that for the corresponding Ru-L-Co series (factor of 5×10^3) (L = iso(Pro)_n, $n = 0-4$) (Table VI). The effect of distance on the rate is seen more clearly in the Os-L-Co series than in the Ru-L-Co series. This is because in the Os-L-Co series the intramolecular electron-transfer rates depend only on preexisting proline conformers (since the electron-transfer rate is either more rapid or of the same order of magnitude as trans to cis proline isomerization). In contrast, in the Ru-L-Co series the rate can be accelerated by preexisting proline conformers as well as conformers formed during the slow electron-transfer process, since the electron-transfer rate is slower than proline isomerization. Therefore, the number of proline conformers which can affect the rate in the Ru-L-Co series is much greater than in the Os-L-Co series.

Based on this analysis, study of even faster electron-transfer systems, where the driving force is increased and/or the reorganization energy of the donor-acceptor set is decreased, should allow further discrimination between the rates for L = iso(Pro)_n, $n = 2-4$. We are currently exploring a series of Os-L-Ru com-

plexes, L = iso(Pro)_n, $n = 2-4$, where such conditions are met.

Acknowledgment. The authors thank Dr. Carol Creutz, Dr. Norman Sutin, and Prof. Henry Taube for helpful discussions. Work done at Rutgers University was supported by the National Institutes of Health Grant GM 26324 and by the National Science Foundation Grant CHE 840552. S.I. is the recipient of a National Institutes of Health Career Development Award (AM 00734) (1980-85) and a Camille and Henry Dreyfus Teacher Scholar Award (1981-85). Work done at Brookhaven National Laboratories is supported by the Office of Basic Energy Science of the Department of Energy.

Registry No. [(NH₃)₅Co-*i*-Os(NH₃)₅](BF₄)₅, 98466-52-5; [(NH₃)₅Co-(Pro)-*i*-Os(NH₃)₅](BF₄)₅, 98481-28-8; [(NH₃)₅Co-(Pro)₂-*i*-Os(NH₃)₅](BF₄)₅, 98466-54-7; [(NH₃)₅Co-(Pro)₃-*i*-Os(NH₃)₅](BF₄)₅, 98466-56-9; [(NH₃)₅Co-(Pro)₄-*i*-Os(NH₃)₅](BF₄)₅, 98466-58-1; [(NH₃)₅Co-*i*-Os(NH₃)₅]⁴⁺, 98466-59-2; [(NH₃)₅Co-(Pro)-*i*-Os(NH₃)₅]⁴⁺, 98466-60-5; [(NH₃)₅Co-(Pro)₂-*i*-Os(NH₃)₅]⁴⁺, 98466-61-6; [(NH₃)₅Co-(Pro)₃-*i*-Os(NH₃)₅]⁴⁺, 98466-62-7; [(NH₃)₅Co-(Pro)₄-*i*-Os(NH₃)₅]⁴⁺, 98466-63-8; [(NH₃)₅Co-(Phe)₂-*i*-Os(NH₃)₅]⁵⁺, 98466-64-9; [(NH₃)₅Co-(Gly)₂-*i*-Os(NH₃)₅]⁵⁺, 98466-65-0; [(NH₃)₅Co-*i*-Ru(NH₃)₄(SO₄)]³⁺, 50914-56-2; [(NH₃)₅Co-(Pro)-*i*-Ru(NH₃)₄(SO₄)]³⁺, 88510-34-3; [(NH₃)₅Co-(Pro)₂-*i*-Ru(NH₃)₄(SO₄)]³⁺, 88524-97-4; [(NH₃)₅Co-(Pro)₃-*i*-Ru(NH₃)₄(SO₄)]³⁺, 88525-00-2; [(NH₃)₅Co-(Pro)₄-*i*-Ru(NH₃)₄(SO₄)]³⁺, 88525-03-5.

Edge-Sharing Biocuboctahedral Dimolybdenum(III) Molecules with μ -RS Groups. Direct Experimental Evidence for Spin-State Equilibria

F. Albert Cotton,^{*1a} Michael P. Diebold,^{1a} Charles J. O'Connor,^{1b} and Gregory L. Powell^{1a}

Contribution from Department of Chemistry and Laboratory for Molecular Structure and Bonding, Texas A&M University, College Station, Texas 77843, and Department of Chemistry, University of New Orleans Lakefront, New Orleans, Louisiana 70148. Received June 5, 1985

Abstract: A series of dimolybdenum(III) molecules with edge-sharing biocuboctahedral structures and general formula (LL)-MoCl₂(μ -SR)₂MoCl₂(LL) have been prepared: namely—**1**, LL = dto, R = Et; **2**, LL = dmpe, R = Et; **3**, LL = dtd, R = Et; **4**, LL = dto, R = Ph; **5**, LL = dmpe, R = Ph; **6**, LL = dtd, R = Ph (dto = EtSCH₂CH₂SEt; dtd = PrSCH₂CH₂SPR; dmpe = Me₂PCH₂CH₂PMe₂). Principal methods of preparation are (a) Mo₂Cl₈⁴⁻ + 2LL + RSSR and (b) Mo₂Cl₄(LL)₂ + RSSR. Compounds **1** and **2** have been structurally characterized by X-ray crystallography. In each case there is a central, planar (LL)Mo(μ -SR)₂Mo(LL) unit with chlorine atoms above and below this plane on each molybdenum atom. Compound **1** forms crystals in space group *C2/c* with $a = 18.114$ (4) Å, $b = 9.925$ (1) Å, $c = 16.403$ (4) Å, $\beta = 97.76$ (2)°, $Z = 4$. The Mo-Mo distance is 2.682 (1) Å. Compound **2** forms crystals in space group *Pnmm* with $a = 12.835$ (3) Å, $b = 15.705$ (5) Å, $c = 9.046$ (2) Å, $Z = 2$. The Mo-Mo distance is 2.712 (3) Å. Compounds **1**, **2**, and **4** have been characterized magnetically and exhibit temperature-dependent magnetic properties consistent with the thermal population of an excited triplet state based on the $\delta^*\delta$ configuration.

Complexes containing two metal atoms that are held in proximity within a set of ten ligand atoms defining an edge-sharing biocuboctahedron afford an opportunity to study metal-metal interactions as many ligand properties are varied. The situation is attractive because of the practical possibilities that exist for systematically controlling and manipulating the circumstances in which these interactions occur, provided of course that synthetic methods can be devised to generate the desired sets of ligands surrounding a given pair of metal ions. This type of structural situation is deserving of study because it is found very commonly in coordination chemistry and solid-state chemistry.

In these laboratories we are engaged in developing synthetic methods that will provide designed access to new M₂L₁₀ species and also in carrying out the structural, spectroscopic, magnetic, and theoretical studies necessary to develop an understanding of the consequent M-M interactions. In this paper we report in detail on the preparation and characterization of dimolybdenum(III) compounds containing bridging RS⁻ groups (R = Et, Ph). Not only are these the first such compounds to be reported, but the synthetic method, viz., oxidative addition to Mo-Mo quadruple bonds, is both novel and capable of being generalized. We also give detailed experimental results and analysis of the magnetic properties of three of these complexes. Portions of this work have been previously published in a preliminary communication.²

(1) Texas A&M University. (b) University of New Orleans.